



CHARACTERISATION OF PLASMA SPRAYED NiCrAlY, Ni-20Cr AND Ni₃Al COATINGS ON A Ni-BASED SUPERALLOY INCONEL 718

S. B. Mishra, S. Prakash, K. Chandra

*Department of Metallurgical & Materials Engineering, Indian Institute of Technology Roorkee,
Roorkee-247 667, INDIA*

ABSTRACT

In the present study the NiCrAlY, Ni-20Cr and Ni₃Al metallic coatings were deposited on a Ni-based Superalloy, namely Inconel 718 (Inconel 718) by Shrouded Plasma Spray Process. NiCrAlY was used as bond coat in all the cases. All the coatings have shown lamellar structure with distinctive boundaries along with the presence of some porosity. The microhardness of the coatings is found to vary with the distance from the coating-substrate interface. Ni-20Cr coating had indicated a maximum microhardness, while a minimum by Ni₃Al coating. The phases revealed by XRD of the coatings have shown the formation of solid solutions.

Keywords : plasma spray coatings, superalloy, protective coatings, NiCrAlY coatings, and erosion.

1. INTRODUCTION

Erosion and high temperature oxidation by the impact of fly ashes and unburned carbon particles are the main problems in heat exchanger tubes and other structural materials in coal-fired boilers^{1,2}. Gas and steam turbines operate in the environments where the ingestions of solid particles are inevitable and results in erosion of materials. In the recent times gas turbine technology for power generation and for aero engine applications places an increasing demand on the use of high temperature Ni-based superalloys e.g. for highly-loaded turbine blades. Although the Ni-base superalloys possess adequate strength at the turbine operating temperatures, they often lack resistance to the combustion environments. In such environments protective coating on the surface of superalloys are frequently used^{3,4}.

Thermally sprayed coatings are widely used in various applications (air crafts, textile, automobile, mining, etc.) to combat various surface degradation processes such as erosion, wear, corrosion, etc.⁵. Today turbine blades and other components of aircraft engines are coated with wear, corrosion and temperature resistant coatings but the science base for this technology is still poorly established and for certain aspects virtually non-existent. The advantages of thermal spraying are that it is relatively inexpensive, part size is not a concern and deposition rate is high^{6,7,8}.

The MCrAlY bond coat provides a rough surface for mechanical bonding of the ceramic top coat, protect the underlying alloy substrate against high temperature oxidation corrosion and minimises the effect of coefficient of thermal expansion mismatch between the substrate and the ceramic top coat materials^{9,10,11}.

Modern thermal spray processes such as high-velocity oxyfuel and plasma spraying are often applied to deposit high-chromium, nickel chromium coatings onto outer surface of various parts

of boilers, e.g. tubes, to prevent the penetration of hot gases, molten ashes and liquids to less noble carbon steel boiler tube¹².

Nickel aluminide has been claimed to possess high-temperature mechanical strength, as well as oxidation resistance^{13,14}. Chuanxian et al¹⁵ and Liao et al¹⁶ has reported wide use of cermet (WC/Co) thermal spray coatings in wear situations because they combine several advantages such as resistance to abrasion, erosion, high temperature and corrosive atmospheres. Singh & Prakash¹⁷ studied the corrosion behaviour of plasma-sprayed Ni₃Al coatings on boiler steels in oxidation and molten salt environments at 900°C and found these coatings are quite effective in developing hot corrosion resistance.

2. EXPERIMENTAL PROCEDURE

2.1 Development of coatings

2.1.1 Substrate material

The substrate material selected for the study was Superni 718 being procured from Mishra Dhatu Nigam Limited, Hyderabad (India) in the rolled sheet form. The chemical composition of the substrate material is 18.5Fe-19Cr-0.15Cu-0.5Al-3.05Mo-0.18Mn-0.9Ti-0.18Si-0.04C-5.13(Cb+Ta) and balance Ni. The specimens each measuring approximately 30mmX30mmX5mm were cut from the sheet. The specimens were polished and grit blasted with alumina powders (grit 60) before being plasma sprayed.

2.1.2 Coating powders

Three types of coating powders for plasma spraying were used in this study. The first powder i.e. Ni₃Al was prepared by mixing nickel (minimum assay 99.5%) and aluminium (minimum assay 99.7%) fine powders in a stoichiometric ratio of 3:1 in the laboratory ball mill for 8 hours to form uniform mixture. The second powder viz. Ni-22Cr-10Al-1Y was also used as a bond coat in all the coatings before applying the final coatings of Ni₃Al, Ni-22Cr-10Al-1Y and Ni-20Cr alloy powders on the specimens.

2.1.3 Coating formulation

Specimens were grit blasted before plasma spraying. 40kW Miller (USA) Thermal Plasma Spray Apparatus was used to apply the coatings. Argon was used as powder carrying and shielding gas. All the process parameters including the spray distance were kept constant throughout the coating process. The parameters include arc current of 700A, arc voltage 35 V, powder flow rate 3.2 rev. /min, spraying distance 90-110 mm, the plasma arc gas and carrier gas pressures of 59 and 40 psi respectively.

2.2 Characterisation of Coating

The microstructural features of the coated specimens were studied using standard metallographic techniques. Scanning Electron Microscope (LEO 435VP) was used to study the surface morphology of the specimens and SEM attached with Robinson Back Scattered Detector (RBSD) was used to obtain the Back Scattered Electron Image (BSEI) along the cross-section of the as sprayed coatings. Zeiss Axiovert 200 MAT Inverted optical microscope fitted with imaging software Zeiss AxioVision Release 4.1, Germany was used for optical microscopy and measurement of porosity of the coated samples. X-ray diffraction (XRD) analysis of the coating in as-sprayed condition was carried out with Bruker AXS D-8 Advance Diffractometer (Germany) with CuK_α radiation. JXA-8600M Electron Probe Micro Analyser (EPMA) was used

to obtain X-ray elemental mapping of the coatings along the cross-section. Microhardness of the coatings is measured by Leitz's Hardness Tester Mini Load-2, Made in Germany. 15 Pond (147.1mN) load was provided to the needle for penetration and hardness value was based on the relation

$$H_v = 1854.4 \times P/d^2$$

(Where P is load in Pond and d is the mean of the indentation diagonal length in mm).

3. RESULTS

3.1 Measurement of Coating Thickness, Porosity and Microhardness of the as plasma sprayed coatings

Figure 1 presents the Back Scattered Electron Images along the cross-section for the plasma sprayed coatings on superalloy Superni 718. The thickness, porosity and microhardness of the coatings measured are compiled in Table 1. The porosity of the plasma sprayed coatings was found to be in the range of 1.46-4.68%. The microhardness profiles of different plasma sprayed coatings are shown in fig. 2. Also the range is given in table 1. The microhardness of substrate superni 718 is found to be in the range of 424-568 Hv.

3.2 Microstructures of plasma sprayed coatings

The surface optical microstructures of different plasma sprayed coatings on superalloy Superni 718 is shown in Fig. 3. Optical micrograph for NiCrAlY (Fig 3a) coating shows small globules distributed along irregular shaped crystals. Some partially melted round particle are seen in the microstructure of as-sprayed Ni-20Cr coating. There is certain directionality indicated by the matrix phase. Fig. 3(b) depicts the microstructures of the Ni-20Cr coated superalloys which are typical for a shrouded plasma spray process. Optical micrographs of the Ni₃Al coatings on different superalloy substrates are shown in Fig. 3(c). It can be seen that the deposited coating is having massive structure indicating large size splats which form the matrix with voids and unmelted oxides.

The optical microstructures along the cross-section of the three plasma sprayed coatings are shown in fig. 4. The as-coated structure is lamellar with some unmelted particles, oxide inclusions and pores. Generally lamellar structure of the coating is evident.

3.3 X-ray diffraction (xrd) analysis

The surface XRD analysis for the coating has been performed using Cu as target. Fig.5 show the XRD patterns for Ni-22Cr-10Al-1Y, Ni-20Cr, and Ni₃Al coating on Superni 718 substrate in the as sprayed condition. γ (Ni) was the major phase observed in all the coatings while in NiCrAlY and Ni₃Al coatings, γ' (Ni₃Al) phase is mainly observed.

3.4 Sem Analysis

SEM micrographs showing surface morphology of the coatings have been depicted in Fig.6. Fig. (a), (b) & (c) shows the as sprayed NiCrAlY, Ni-20Cr and Ni₃Al coatings, respectively on superni 718 superalloy substrate. Plasma sprayed coating was formed with the presence of layering and stacking of the layers in the coating. This was caused when the melted powder particles were deposited in the form of light and dark layers and the non-melted and partly melted particles appeared as spherical or round shape with non-uniform deposition in the coatings. Also some splats formed in the coating can be seen in the SEM micrographs. The SEM analyses of the coatings show that during all regimes of spraying the bonding between the superalloy substrate and coating was very good, without cracks or other defects.

3.5 Electron Probe Micro Analysis (Epma)

The EPMA analysis from the cross-sectional BSEI of the as-sprayed NiCrAlY coating shows distinct layers of the coating and the substrate (Fig. 7). X-ray mappings of the different elements for this coating show no significant diffusion of elements from the substrate to the coating layer. Minor diffusion of iron, tantalum, titanium and manganese has been indicated. The elements of the coating viz. Ni, Cr, Al and Y have indicated uniformly distribution within the coating region. There is a band just above the substrate in the coating where Ni and Cr mainly exists and aluminium is absent.

Fig.8 depicts the cross-sectional BSEI of the as-sprayed Ni-20Cr coating with different layers. The top region represent the Ni-20Cr coating, the intermediate region is the bond coat and the lower area the substrate. The Ni-20Cr coating is dense as compared to the bond coating. The elements of substrate, coating and bond coat are mainly confined to their original places except aluminum and to some extent titanium, tantalum, iron and manganese. Aluminum has shown significant diffusion to the Ni-20Cr coating region especially at the places where Ni is absent. Ti, Ta, Fe and Mn have also been noticed in small but uniformly distributed concentration in the top coat as well as in the bond coat. This indicates probable diffusion of these elements from the substrate superalloy.

X-ray mappings for the Ni₃Al coating as depicted in Fig. 9 indicate noticeable diffusion of titanium and tantalum from the substrate to Ni₃Al coating and bond coat. Equally distributed traces of iron and manganese could be seen in the coating as well as in the bond coat. Bond coat/substrate interface is evident.

4. DISCUSSIONS

The measured values of porosity for the coatings are almost in agreement with the findings of Demirkiran et al¹⁸, Sidhu¹⁹, Miguel et al²⁰, Chen et al²¹, Erickson et al²² and Hidalgo et al^{23,24}. The microhardness values of the coatings have been compared with those reported by Miguel et al²⁰, Sundararajan et al²⁵, Mateos et al²⁸, Hoop et al², Staia et al²⁷, Hidalgo et al²⁸, and Sampath et al²⁹ and are found to be in similar range. Robert Jr.³⁰ has also reported extensive data on properties of plasma coatings and values of porosity and microhardness data have been found to be similar to those published by him. Further increase in microhardness of the substrate has been observed near the coating-substrate interface. This substrate hardening may be arising from the high speed impact of the coating particles during plasma spray deposition. The phenomenon has also been observed by Sidhu¹⁹, Hidalgo et al^{23,24} and Sidhu & Prakash¹⁷. Staia et al²⁷ have reported different values of microhardness in case of plasma sprayed Cr₃C₂-25%NiCr coatings for carbide plus carbo-nitride phase and the Ni-Cr matrix present in the same coating. Moreover the microhardness and other properties of the thermal spray coatings are anisotropic because of their typical splat structure and directional solidification³⁰.

Sampath et al²⁹ explained the formation of splats in case of air plasma sprayed coating of Ni-5 wt% Al bond coat. They observed that the core of the splats is predominantly nickel, whereas the aluminium, because of its tendency to oxidise is concentrated towards the outer surface of the splats i.e. splat boundaries. Microstructures similar to those of present study i.e. lamellar structures with voids and oxide inclusions have also been reported by Sidhu¹⁹, Erickson et al²², Sampath et al²⁹, Bluni and Mardar³¹, Hsu and Wu³², Westergard et al³³, Ilavsky et al³⁴, Rosso et al³⁵, Margadant et al³⁶, and Choi et al³⁷. Wigren and Tang³⁸ opined that the microstructure of a thermally sprayed coating typically consists of a multiphase matrix (often a mix between hard, soft and amorphous), pores, oxides, delaminations, cracks, and unmelted particles.

The presence of γ -Ni and γ' -Ni₃Al as main phases in NiCrAlY coatings has also been reported by Sidhu¹⁹ for shrouded plasma sprayed NiCrAlY coatings. From these phases, it can be inferred that the structure of the NiCrAlY coating consists mainly of γ (nickel solid solution) and γ' (Ni₃Al). Wu et al³⁹ have also reported the similar structure of plasma sprayed NiCrAlY coatings. The γ -Ni phase shown by XRD of as sprayed Ni-20Cr coating might be indication of formation of nickel solid solution matrix in the coating.

In case of Ni₃Al coating, the formation of Ni₃Al as a main phase has been confirmed by XRD. The similar XRD peaks have also been reported by Sidhu & Prakash¹⁷, Singh¹⁹, La et al⁴⁰ and Liu and Gao⁴¹. Further the method of preparation of Ni₃Al powder for the present study had also been used by Sidhu & Prakash¹⁷, Sidhu et al¹⁹, and La et al⁴⁰.

It has been observed from the EPMA (Fig. 4.7 through 4.9) that the chances of interdiffusion of various elements between the substrate and plasma sprayed coatings are very less. However in relative terms the diffusion between the bond coat and top coat is found to be more likely to occur. Quantitatively aluminium is found to be the most vulnerable element to the diffusion phenomenon. Cr, Ti, Ta, Fe and Mn are some other elements which are prone to minor diffusion. Nicholls⁴² has opined that diffusion of elements between the substrate and coating can have a major influence on coating performance. Therefore to provide long-term stability at elevated temperatures, it is necessary to develop diffusion-barrier coatings to minimize the interdiffusion between the coating and the substrate. However, he further added that some interdiffusion is necessary to give good adhesion; hence, the diffusion barriers must be tailored to limit the movements of particular problematic elements.

5. CONCLUSIONS

1. The porosity of the coatings has been found to be in the range 1.46-4.68%. The microhardness values are shown in table 2. The microhardness of substrate superalloy 718 is found to be in the range of 424-568 Hv.
2. γ (Ni) was the major phase observed in all the coatings while in NiCrAlY and Ni₃Al coatings, γ' (Ni₃Al) phase is mainly observed. The γ -Ni phase shown by XRD of as sprayed Ni-20Cr coating might be indication of formation of nickel solid solution matrix in the coating.
3. The SEM analyses of the coatings show that during all regimes of spraying the bonding between the superalloy substrate and coating was very good, without cracks or other defects.
4. The as-coated structure is lamellar with some unmelted particles, oxide inclusions and pores.
5. X-ray mappings of the different elements for this coating show no significant diffusion of elements from the substrate to the coating layer. Minor diffusion of iron, tantalum, titanium and manganese has been indicated.

REFERENCES

1. Hidalgo V H, Varela F J B, and Rico E F, *Tribology International*, 30 (1997) 641.
2. Hoop P J and Allen C, *Wear* 233-235 (1999) 334.
3. Tabakoff W, *Surface and Coatings Technology* 120-121 (1999) 542.
4. Stroosnijder M F, Mevrel R, and Bennett M J, *Materials at High Temperature* 12 (1994) 53.
5. Murthy J K N, Rao DS, and Venkataraman B, *Wear* 249 (2001) 592.
6. Hocking M G, *Surface and Coatings Technology* 62 (1993) 460.
7. Pfender E, *Surface and Coatings Technology* 34 (1988) 1.
8. Branco J R T, Gansert R, Sampath S, Berendt C C and Herman H, *Materials Research*, 7/1 (2004) 147.
9. Eliaz N, Shemesh G and Latanision R M, *Engineering Failure Analysis* 9 (2002) 31.

10. Hussain N, Shahid K A, Khan I H, and Rahman S, *Oxidation of Metals* 41 (3/4) (1994) 251.
11. Zhao H X, Goto H, Matsumura T, Takahashi T, and Yamamoto M, *Surface and Coatings Technology* 115 (1999) 123.
12. Tuominen J, Vuoristo P, Mantyla T, Ahmaniemi S, Vihinen J, and Andersson P H, *Journal of Thermal Spray Technology* 11(2) (2002) 233.
13. He J L, Chen K C, Chen C C, Leyland A, and Matthews A, *Surface and Coatings Technology* 135 (2001) 158.
14. Schneibel J H, and Becher P F, *J. Chinese Inst. Engg.* 22 (1) (1999) 1.
15. Chuanxian C, Bingtang H, and Huiling L *Thin Solid Films* 118 (4) (1984) 485.
16. Liao H, Normand B, and Coddet C, *Surf. Coat. Technol.* 124 (2000) 235.
17. Sidhu B S, and Prakash S, *Surface & Coatings Technology* 166 (2003) 89.
18. Demirkiran A S, Avci E, *Surface and Coatings Technology*, 116-119 (1999) 292.
19. Sidhu B S, *Ph.D. Thesis*, Metallurgical & Materials Engineering Department, Indian Institute of Technology Roorkee, India (2003).
20. Miguel J M, Guilemany J M, and Vizcaino S, *Tribology International*, 36 (2003) 181.
21. Chen H C, Liu Z Y, Chuang Y C, *Thin Solid Films*, 223 (1993) 56.
22. Erickson L C, Westergard R, Wiklund U, Axen N, Hawthorne H M, and Hogmark S, *Wear* 214 (1998) 30.
23. Hidalgo V H, Varela F J B, and Menendez A C, *Proc. of 15th Int. Thermal Spray Conference*, Nice, France (1998) 617.
24. Hidalgo V H, Varela F J B, Martinez S P, and Espana S G, *Proc. of the United Thermal Spray Conference*, Germany (1999) 683.
25. Sundararajan T, Kuroda S and Abe F, *Materials Transactions* 45(4) (2004) 1299.
26. Mateos J, Cuetos J M, Vijande R, and Fernandez E, *Tribology International* 34 (2001) 345.
27. Staia M H, Valente T, Bartuli C, Lewis D B, Constable C P, *Surface and Coatings Technology* 146-147 (2001) 553.
28. Hidalgo V H, Varela J B, Calle J M, and Menendez A C, *Surface Engineering* 16 (2000) 137.
29. Sampath S, Jiang X Y, Matejcek J, Prchlik L, Kulkarni A, and Vaidya A, *Materials Science and Engineering A* 364 (2004) 216.
30. Tucker R C Jr., *Advanced Thermal Spray Deposition Techniques*, Handbook of Deposition Technologies for Films & Coatings, Eds. R.F. Bunshah, William Andrew Publ./Noyes (1994) p 617.
31. Bluni S T, and Marder A R, *Corrosion* 52 (3) (1996) 213.
32. Hsu I C and Wu H K, *Surface and Coatings Technology* 90 (1997) 6.
33. Westergard R, Erickson L C, Axen N, Hawthorne H M, and Hogmark S, *Tribology International* 31(5) (1998) 271.
34. Ilavsky J, Pisacka J, Chraska P, Margadant N, Siegmann S, Wagner W, Fiala P, and Barbezat G, *Proceedings of the International Thermal Spray Conference* (2000) 449.
35. Rosso M, Ugues D, Becgis F, Groppetti R, Scrivani A, Bardi U and Rizzi G, *Proceedings of the International Thermal Spray Conference* (2001) 75.
36. Margadant N, Siegmann S, Patscheider J, Keller T, Wagner W, Ilavsky J, Pisacka J, Barbezat G, and Fiala P, *Proceedings of the International Thermal Spray Conference* (2001) 643.
37. Choi H, Yoon B, Kim H, Lee C, *Surface and Coatings Technology* 150 (2002) 297.
38. Wigren J, and Tang K, *Proceedings of the International Thermal Spray Conference* (2001) 1221.
39. Wu Y N, Zhang G, Feng Z C, Zhang B C, Liang Y, and Liu F J, *Surface and Coatings Technology* 138 (2001) 56.
40. La P, Bai M, Xue Q, and Liu W, *Surface and Coatings Technology* 113 (1999) 44.
41. Liu Z, Gao W, *Oxidation of Metals* 55 (5-6) (2001) 481.
42. Nicholls J R, *JOM* 52(1) (2000) 28.

TABLES

Table 1 Average coating thickness, porosity and microhardness of as-sprayed plasma coatings.

Coating	Coating Thickness (μm)			Porosity (%)	Microhardness (Hv)
	Bond coat (NiCrAlY)	Outer coat	Total		
NiCrAlY	-	-	398	1.95-4.48	404-568
Ni-20Cr	104	220	324	2.99-4.68	385-611
Ni ₃ Al	168	305	473	1.46-3.99	230-344

FIGURES

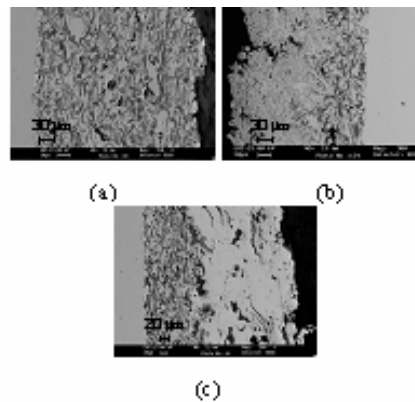


Fig.1 Scanning electron micrograph showing cross-sectional morphology of as sprayed plasma coatings on Superalloy 718 (a) NiCrAlY, (b) Ni-20Cr and (c) Ni₃Al

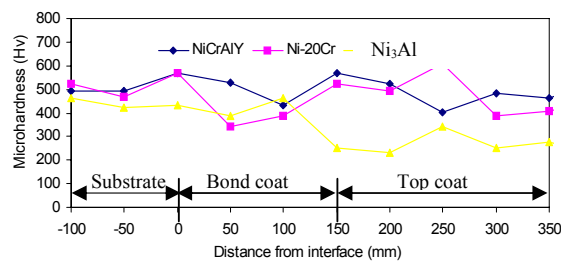


Fig. 2 Microhardness profiles of different as sprayed coatings with bond coat of NiCrAlY for Superalloy 718 substrate along the cross-section.

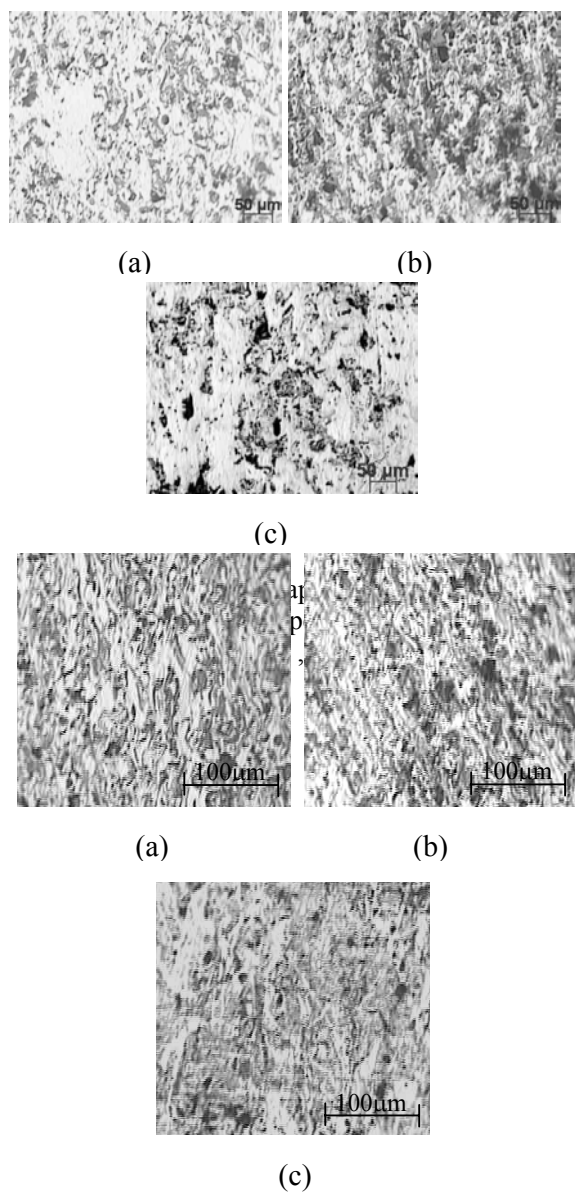


Fig. 4 Optical micrograph along the cross-section of different plasma sprayed coatings on Superni 718 (a) NiCrAlY, (b) Ni-20Cr, (c) Ni₃Al.

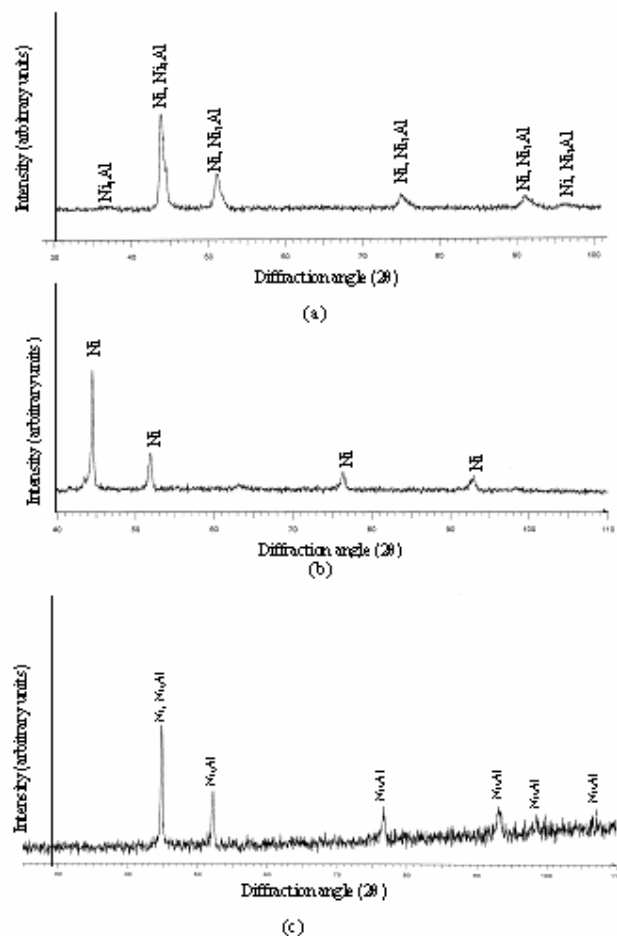


Fig. 5 X-ray diffraction patterns for the plasma sprayed coatings on superalloy Superalloy 718
 (a) NiCrAlY coated
 (b) Ni-20Cr coating with bond coat
 (c) NiAl coating with bond coat

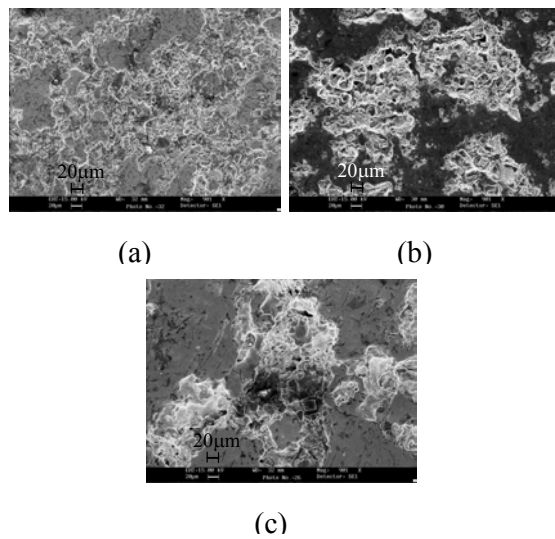


Fig.6 Scanning electron micrograph of as sprayed plasma coatings on superalloy 718 (a) NiCrAlY, (b) Ni-20Cr and (c) Ni₃Al

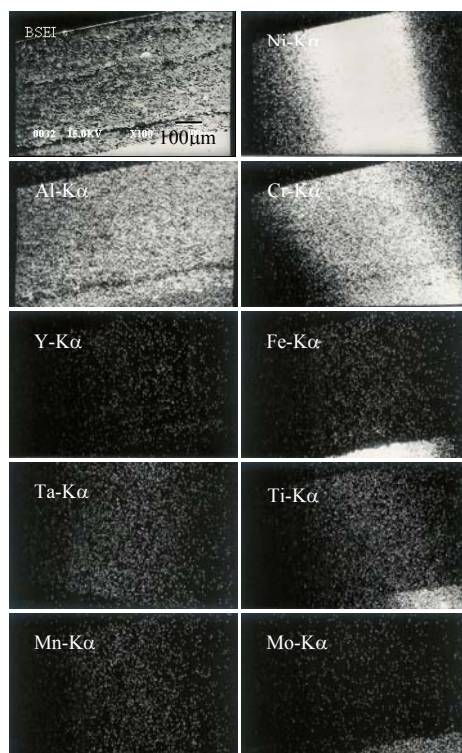


Fig.7 BSEI and elemental X-ray mapping of the cross-section of plasma sprayed NiCrAlY coating on Inconel 718 superalloy.

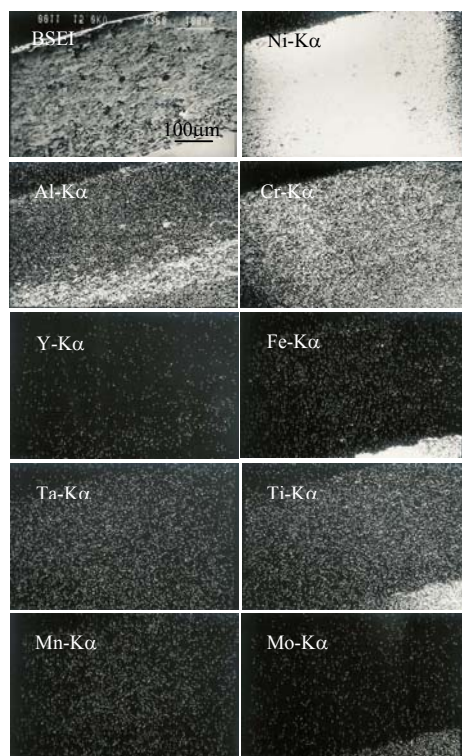


Fig.8 BSEI and elemental X-ray mapping of the cross-section of plasma sprayed Ni-20Cr coating with bond coat of NiCrAlY on superalloy 718



Fig9 BSEI and elemental Xray mapping of the cross-section of plasma sprayed NiAl coating with bond coat of NiCrAlY on superalloy 718 superalloy.